An experimental and detailed chemical kinetic investigation of the addition of C2 oxygenated species in rich ethylene premixed flames

Z. Malliotakis[1], N. Leplat[2], G. Vourliotakis[1,*], Ch. Keramiotis[1], G. Skevis[3], M.A. Founti[1], J. Vandooren[2]

[1]Laboratory of Heterogeneous Mixtures and Combustion Systems, School of Mechanical Engineering, National Technical University of Athens, Greece
[2]Laboratoire de Physico-Chimie de la Combustion, Université Catholique de Louvain, Louvain-la-Neuve, Belgium
[3]Aerosol and Particle Laboratory, Chemical Processes and Energy Resources Institute, Centre for Research and Technology Hellas, Thessaloniki, Greece

Abstract

Current needs for reduced emissions and improved efficiency have motivated the study of the combustion chemistry of novel fuels. In particular, in the automotive industry, the addition of oxygenated fuels as components in commercial fuels, or even as neat fuels, is being increasingly considered. The aim of this work is to analyse the effect of the addition of three C2 oxygenated species namely, acetaldehyde, ethanol and acetic acid, representative of three different fuel classes in rich ethylene premixed flames and to quantify the influence of these oxygenated species on the flame structure. All flames are kept at a constant C/O ratio of 0.75. Experimental results highlight the important role played by ketene, acetaldehyde and vinyl alcohol as intermediates. The kinetic schemes of the research groups (NTUA and UCL) co-authoring the study are used and further analysed. Both mechanisms appear to satisfactorily reproduce flames structure. Reaction path analysis is extensively utilized in order to scrutinize the controlling elementary steps and to highlight areas of the mechanism needing further improvement.

Introduction

The continuous increase in energy consumption and concerns about fossil fuels availability, together with the current trends in novel IC engines development, call for further research on alternative fuels [1]. Such fuels, may also be renewable, and may include smaller fuel molecules with possible oxygenated content, such as syngas and small alcohols [2].

Ethanol is particularly attractive as an alternative fuel due to its soot and emissions reduction potential and is often found as an oxygenated additive compound in gasoline fuels [3]. Fundamental research on the oxidation of conventional fuel/alcohol blends has determined aldehydes, such as acetaldehyde, as important intermediate species. Aldehydes are products of partial/ incomplete combustion and, being stable intermediates they influence the combustion pathways. Additionally, studies on engines [4, 5] have shown that, depending on the engine operating conditions, up to 4-27% of the exhaust hydrocarbons are acids, mainly acetic and proprionic acid, which have also been recognised as contributors to acid rain formation. All the above constitute the research of the respective oxygenated families and species of high importance.

The study of ethylene is of significant interest, as it is a key intermediate of the oxidation of higher alkanes, and a very reactive fuel as well. It is often used as a model fuel for soot studies [6].

Given the limited information and the experimental uncertainty from the combustion in engines and practical propulsion devices, one has to obtain knowledge using fundamental lab-scale configurations, such as premixed flames, ignition delay time in shock tubes, flame velocity measurements etc. Studies on flame structure in particular, can in principle provide greater insight on the fundamentals of the combustion process itself, by providing a rudimentary description of the flow-chemistry interaction encountered in real combustion applications, but giving high insight on the details of chemistry.

Several relevant experiments have been carried out in the past by different research groups. Among them, Yakimov *et al.* [7] measured product species in a premixed laminar ethylene flame at low pressure, with and without the addition of ethanol. Results yielded a reduction of soot precursor species such as C_3H_3 and C_6H_6 and other intermediate species as well. Additionally, Xu *et al.* (2012) [8] investigated the addition of alcohols, such as ethanol and methanol, in a n-heptane/toluene premixed laminar flame at low pressure. The study showed trivial effects on fuel consumption, but reduced formation of intermediate aromatic hydrocarbons, lowering thus soot emissions.

The scope of the present study is to quantify the effect of oxygenated species additives on the structure of rich ethylene premixed flames. The kinetic scheme of NTUA [9, 10], and the detailed kinetic model of UCL [11-16], are utilized and further analyzed towards the development of a detailed reaction model able to accurately describe the combustion chemistry of C2 oxygenated species. The NTUA model has been extensively validated against experimental speciation data from C1-C6 counterflow and premixed flames, including laminar flame speeds, shock tubes, including

* Corresponding author: gvou@central.ntua.gr

ignition time delays, as well as from perfectly stirred and plug flow reactors, all under a wide range of temperatures, pressures, and stoichiometries. The kinetic mechanism of UCL has been obtained by merging the model built and validated against experiments relevant to ethanol, acetaldehyde and acetic acid combustion [11-14] for the H_2/O_2 system and carbonated compounds up to 3 carbon atoms, with the scheme assembled and validated against Benzene and Toluene experiments by Detilleux and Vandooren [15, 16] for heaviest species (up to C_{12}).

Experimental setup

All experiments have been conducted in the facilities of the UCL. Detailed description of the experimental setup can be found in [15, 16] and only a brief description is provided herein. The experimental setup consists of a gas chromatographer (GC) coupled to a combustion chamber. A cooled brass, sintered plate, flat flame burner of 8 cm diameter lies in the low pressure combustion chamber. Flames A and B were stabilized at 50 mbar whereas measurements in Flame C were made at 75 mbar. The latter flame was found to be positioned too far from the burner at 50 mbar and subsequently had a tendency to blow off. A conical quartz probe allows sampling from the flame. The sampling position is controlled by moving the burner, thus altering the distance between the burner and the sampling probe.

An accurately controlled amount of the sampled gases were trapped in a cylinder before being compressed by means of a piston. The compressed gases were introduced into the GC in which a chromatographic discrimination was achieved by using either a Molsieve 5A (H_2, O_2 and CO) or a PORAPLOT Q (other hydrocarbons) column provided by Varian Inc. The quantification detection was carried out by both a Thermal Conductivity Detector (TCD) and Flame Ionization Detector (FID) previously calibrated by the procedure described in a earlier paper [15].

Flame temperatures were measured using Pt/PtRh10% coated thermocouples of 0.1 mm diameter, placed in front of the sampling probe, at a distance of 0.3-0.5 mm. Correction of radiation losses was carried out by the electrical compensation method. Standard deviation on temperature measurements is estimated to ±50 K. The experimental temperature profiles for the three flames are shown in Fig. 1. The measured maximum temperatures are between 1750 and 1800 K in all investigated flames, however differences up to 300 K can be found in the reaction zone.

The composition of the investigated flames is listed in Table 1. In all the flames, the initial ethylene, as well as the initial oxygenated additive molar concentration, have been held constant, namely 0.25 and 0.08 respectively. The molecular oxygen content is held constant in the acetaldehyde and the ethanol flame but is decreased in the acetic acid flame in order to maintain constant the C/O ratio. The diluent (Ar) content rises instead.

Concentration profiles for the following species have been measured for all three flames: H_2, O_2, CO (carbon monoxide), CO_2 (carbon dioxide), H_2O, C_2H_2+C_2H_4 (acetylene + ethylene), CH_4 (methane), C_2H_6 (ethane), C_3H_6 (propene), C_3H_8 , CH_2CCH_2 (allene), $CHCCH_3$ (propyne), CH_3CHO (acetaldehyde), CH_3COOH (acetic acid), C_2H_5OH (ethanol), C_4H_4 (vinylacetylene), C_4H_6, C_4H_2, C_5H_6 (cyclopentadiene), C_6H_6 (benzene), C_7H_8 (toluene).

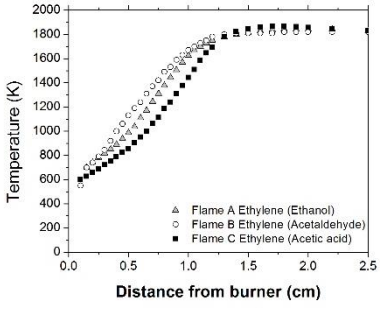

Figure 1 Measured temperature profiles for all three flames.

Numerical approach

The detailed kinetic schemes of the two research groups have been utilized to compute the experimentally investigated flames. Both mechanisms have been extensively validated against speciation data from premixed flames of both small H/C and C1-C2 oxygenated species, e.g. for the NTUA mechanism see [9, 10], for the UCL mechanism see [11-16]. Additionally, the UCL mechanism was developed in part to simulate experimental data coming from C_6H_6 and C_7H_8 flames [15, 16]. Currently, the NTUA mechanism comprises of 145 species among 849 elementary reactions while the respective figures for the UCL mechanism are 174 and 891.

All computations have been performed using the PREMIX code [17]. The experimentally determined temperature profiles have been imposed to calculations, so that heat losses to the burner are explicitly taken into account. The multi-component diffusion model was mostly used, and grid adaptation parameters have been chosen so as to insure high grid resolution and grid-independent solutions. More information about the numerical methodology can be found in [9, 14]

Reaction path analysis is extensively utilized in order to scrutinize the controlling elementary steps and the combustion pathways of the three oxygenated additives among ethylene are discussed and reassessed. Parts of the mechanism are identified for further models improvement, based on critical evaluation of the experimental data and the available specific rate constants.

Primary fuel destruction paths and major products

The detailed kinetic oxidation of ethylene has already been studied in many previous works, e.g. [18- 21], and will therefore, not be discussed in full detail here. Since there are not direct C_2H_4 measurements, Fig. 2 presents a comparison between computed and measured fuel decay profile of a previously published rich ethylene flame [18], where both mechanisms are shown to achieve good agreement.

In all flames ethylene is mainly consumed (75% of total ethylene destruction) to the vinyl radical by hydrogen abstraction (reactions R1 and R2 at a relative

ratio 3:2) for both mechanisms. A small amount of fuel is converted to the oxygenated 2-oxoethyl (CH_2CHO) via reaction R3.

$C_2H_4+H<=>C_2H_3+H_2$ (R1)
$C_2H_4+OH<=>C_2H_3+H_2O$ (R2)
$C_2H_4+O<=>CH_2CHO+H$ (R3)

The UCL mechanism shows an additional path for ethylene destruction, through methyl radical attack on the fuel, forming vinyl radical and methane with a share of 10%. This reaction, also constitutes as the second major formation path of methane in Flame A. Both mechanisms are shown to accurately reproduce major species profiles across the flame domain, as it is shown in Figs. 3, 4 and 5 for Flames A, B and C respectively.

Vinyl radical is almost equally consumed to acetylene and CH_2CHO, through its unimolecular decomposition and reaction with O_2 respectively. Recent studies have shown the importance of the competition among the unimolecular decomposition and the reaction with O_2 for key combustion intermediates such as C_2H_3 and HCO [9, 22, 23].

Flame	X_{C2H4}	X_{C2H5OH}	X_{CH3CHO}	$X_{CH3COOH}$	X_{O2}	X_{Ar}	Mass flow rate (g/cm^2 s)	C/O	ϕ	Pressure (mbar)
Flame A	0.25	0.08	-	-	0.4	0.27	2.835 10-3	0.75	2.475	50
Flame B	0.25	-	0.08	-	0.4	0.27	2.822 10-3	0.75	2.375	50
Flame C	0.25	-	-	0.08	0.36	0.31	2.954 10-3	0.75	2.527	75

Table 1. Detailed setup of investigated flames

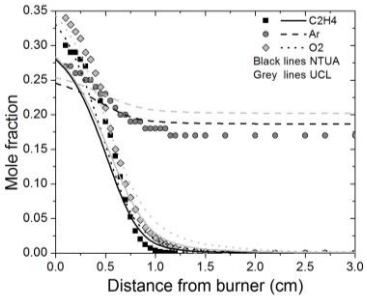

Figure 2 Comparison between experimental data (symbols), and computational results (lines) for reactant species in the flame of [8] (see text).

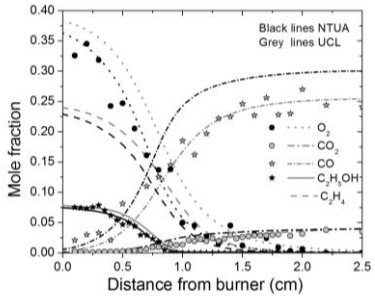

Figure 3 Comparison between experimental data (symbols), and computational results (lines) for major species in Flame A.

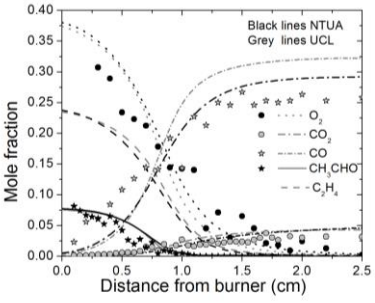

Figure 4 Comparison between experimental data (symbols), and computational results (lines) for major species in Flame B.

Analysis of the mechanisms also confirmed the competitive nature of R5 and R6. As expected, the H abstraction path of C_2H_3 (R4) is the sole acetylene formation route. Acetylene is then decomposed to the ketyl radical (HCCO), which in turn is consumed to CO and CO_2, terminating the combustion process. Formation of CH_2CHO is due to O_2 attack on C_2H_3, while reaction R4 only contributes up to 15%. The destruction of CH_2CHO is realized via its isomerization reaction to the acetyl radical (CH_3CO) and its decomposition to ketene and H_2 at a ratio 3:2.

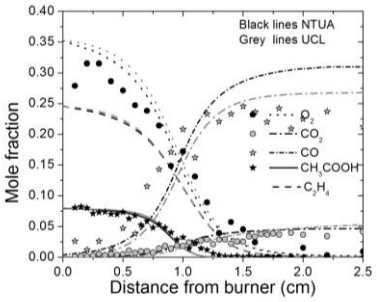

Figure 5 Comparison between experimental data (symbols), and computational results (lines) for major species in Flame C.

$C_2H_3+H<=> C_2H_2+H_2$ (R4)
$C_2H_3(+M)<=> C_2H_2+H(+M)$ (R5)
$C_2H_3+O_2<=> CH_2CHO+O$ (R6)
$C_2H_3+O_2<=>HCO+CH_2O$ (R7)
$CH_2CHO<=>CH_3CO$ (R8)
$CH_2CHO <=>CH_2CO+H$ (R9)

The next step would be to examine the fate of each dopant. In both mechanisms, ethanol is consumed through H abstraction (R10) to the a-hydroxyethyl radical (CH_3CHOH) and decomposition to ethylene and water (R11) starting a bit later in the flame domain. In the NTUA mechanism the former path dominates over the latter with a branching ratio of 2:1, while the USC mechanism predicts a slightly higher contribution of the decomposition path (R11) (thus resulting to higher water levels, as it will be discussed below). In both cases

ethanol decomposition occurs very early in the flame domain and thus some additional ethylene is available in the flame zone. Note also that direct destruction of ethanol to the other two C_2H_5O isomers (b-hydroxyethyl and ethoxy radicals) constitutes only a minor part of its destruction rate.

$C_2H_5OH+H<=>CH_3CHOH+H_2$ (R10)
$C_2H_5OH(+M)<=>C_2H_4+H_2O(+M)$ (R11)

The a-hydroxyethyl radical is transformed to acetaldehyde (R12) and vinyl alcohol (R13), either at equal rates for the NTUA mechanism, or at a ratio of about 20:1 in the UCL model. In flame A, about 35% of acetaldehyde breaks to methyl and formyl radical while the rest is consumed to 2-oxoethyl and acetyl radical through hydrogen abstraction reactions.

$CH_3CHOH+O_2<=>CH_3CHO+HO_2$ (R12)
$CH_3CHOH<=>CH_2CHOH+H$ (R13)
$CH_3CHO(+M)<=>CH_3+HCO(+M)$ (R14)
$CH_3CHO+H<=>CH_2CHO+H_2$ (R15)
$CH_3CHO+H<=>CH_3CO+H_2$ (R16)

On the other hand, when acetaldehyde is a fuel component, it is primarily consumed to the C_2H_3O isomers by reactions with hydrogen and hydroxyl radicals. Once formed, both C_2H_3O isomers destruction follows the paths described earlier. The branching ratio of reactions R15 and R16 between acetyl radical and 2-oxoethyl of the isomers is almost 1:1 in both mechanisms, see also discussion in [9].

$CH_3CHO+CH_3<=>CH_3CO+CH_4$ (R17)
$CH_3CHO+OH<=>CH_2CHO+H_2O$ (R18)
$CH_3CHO+OH<=>CH_3CO+H_2O$ (R19)

Acetaldehyde levels in the acetic acid flame are of the order of 50 ppm, significantly lower than the case of Flame A. Both mechanisms follow the observed trends, the NTUA mechanism is generally a factor of two lower than UCL but within the error bars of the data

Leplat and Vandooren [11] have studied neat acetic acid flames and assembled a relevant sub-mechanism that has been also adopoted in the present study by both mechanisms. Early in the flame, the consumption of acetic acid starts with H abstraction from the methyl group (R21). Consecutively, CH_2COOH forms ketene and a hydroxyl radical through β-scission reaction (R23). Note that ketene levels in Flame C are 5 times higher of those in Flames A and B, with the sole difference in CH_2CO formation rates being the contribution of the acetic acid path (R23). The rest of ketene comes from the unimolecular decomposition of CH_2CHO.

$CH_3COOH+OH<=>CH_2COOH+H_2O$ (R20)
$CH_3COOH+H<=>CH_2COOH+H_2$ (R21)
$CH_2COOH<=>CH_2CO+OH$ (R22)

Ketene is then consumed to the methyl radical (R23) and the ketenyl radical (R24) after being attacked by a hydrogen atom. The branching ratio of the two reactions is 3:2.

$CH_2CO+H<=>CH_3+CO$ (R23)
$CH_2CO+H<=>HCCO+H_2$ (R24)

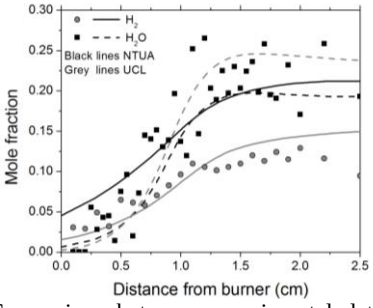

Figure 6 Comparison between experimental data (symbols), and computational results (lines) for H_2 and H_2O in Flame C.

Figure 6 presents computed values and experimental data for H_2 and H_2O. Due to the dominance of C_2H_4 over the C_2 oxygenated additives, H_2 formation is due to R25 and R26 (ratio of about 3:2). In the case of ethanol, the H fuel abstraction path leading to the dominant C_2H_5O isomer (1-hydroxyethyl) also contributes about 10% of the total H_2 formation rate. Similarly, H abstraction reaction of acetaldehyde with H atoms towards C_2H_3O isomers, also results to H_2 formation (at equal rates). Interestingly, despite the high levels of acetaldehyde in the ethanol flame, these reactions do not contribute to H_2 production in Flame A. In Flame C, no additive-specific reaction contributes to H_2 formation. Once formed, H_2 rigorously reacts with hydroxyl radical to form water.

$C_2H_4+H<=> C_2H_3+H_2$ (R25)
$CH_2O+H=HCO+H_2$ (R26)
$C_2H_5OH+H<=>CH_3CHOH+H_2$ (R27)
$CH_3CHO+H<=>CH_3COH+H_2$ (R28)

Key intermediate species chemistry

Figure 7 presents the performance of both mechanisms against the measured values of ethane and propene. Overall, both models result in very good agreement. Ethane formation occurs almost exclusively due to the methyl radical recombination in all flames. This is an important step in the ethylene oxidation, providing a path for nonreactive methyl radicals to produce highly reactive ethyl radicals via H abstraction reactions.

$2CH_3(+M)<=>C_2H_6(+M)$ (R29)

Both mechanisms agree on the propane formation route. Recombination between vinyl and methyl radicals (R30) accounts for approximately 90% of propene formation in Flame A, with similar figures being valid for the other flames. Ethylene and singlet methylene radical react to additionally contribute to propene formation up to 40% of the total rate (R31).

$C_2H_3+CH_3(+M)<=>C_3H_6(+M)$ (R30)
$CH_2(S)+C_2H_4<=>C_3H_6$ (R31)

Propene is destructed via H abstraction reactions. The branching ratio between the channels leading to the allyl radical and to ethylene is of the order of 4:1. Formation of the other two C_3H_5 isomers, namely the 1- 2-methylvinyl radical are also formed through H atoms attack on propene.

$C_3H_6+H<=>a\text{-}C_3H_5+H_2$ (R32)

$C_3H_6 + H <=> C_2H_4 + CH_3$ (R33)
$C_3H_6 + H <=> (1)\text{-}C_3H_5 + H_2$ (R34)
$C_3H_6 + H <=> (2)\text{-}C_3H_5 + H_2$ (R35)

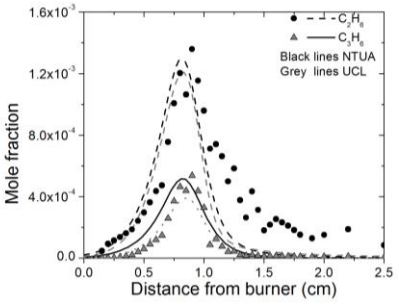

Figure 7 Comparison between experimental data (symbols), and computational results (lines) for C_2H_6 and C_3H_6 in Flame A.

Further downstream in the carbon path, methane (Fig. 8) formation according to the NTUA mechanism is due to the addition reactions of methyl radical with formyl and hydrogen radical. On the contrary, the UCL mechanism adopts addition paths of ethylene with methyl radical and vinyl radical respectively. In Flame C, there is a 10% contribution in the total methane formation rate from fuel decomposition reaction to ethane and carbon dioxide (R36).

$CH_3COOH <=> CH_4 + CO_2$ (R36)

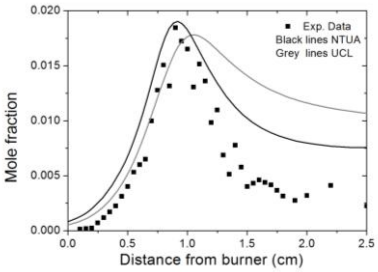

Figure 8 Comparison between experimental data (symbols), and computational results (lines) for CH_4 in Flame A.

Secondary paths in ethylene-oxygenated blends

Vinylacetylene is formed in both mechanisms by addition of a vinyl radical to acetylene. Figure 9 presents mechanisms agreement on measured C4 species in Flame B. The NTUA mechanism is shown to over-predict C_4H_4 levels by a factor of 3, while the UCL model correctly reproduces peak levels. On the other hand the NTUA and UCL mechanism bracket the experimental C_4H_2 data although the species decay in the post flame zone is slower in the case of the former mechanism. Note also that both kinetics schemes are shown to satisfactorily capture the experimental data of butadiene (see Fig. 10).

The C5 chemistry is largely initiated by CH_x radical species addition reaction to either diacetylene or vinylacetylene. For example, the major formation path for cyclopentadiene in the NTUA mechanism, which is the dominant C5 species in all three flames, is triplet methylene addition to vinylacetylene, reaction (R37). The respective path in the UCL mechanism is the one of vinyl radical reaction with propyne. Computed C_5H_6 levels are shown in Fig. 11. Figure 11 shows that cyclopentadiene is over-predicted by the UCL mechanism while NTUA prediction is slightly below the measured data.

$C_4H_4 + CH_2(T) <=> c\text{-}C_5H_6$ (R37)
$C_2H_3 + pC_3H_4 <=> c\text{-}C_5H_6 + H$ (R38)

Benzene formation and molecular growth paths

Benzene formation paths in hydrocarbon flames have been attained much of attention in the literature [24]. In both mechanisms, benzene is mainly formed through vinylacetylene reaction with vinyl radical and another small amount is being formed through addition reactions of phenyl radical with hydrogen. The relative ratio of those paths is 6:1. Benzene destruction to the phenyl radical follows the typical routes of H abstraction reactions with H, OH, and CH_3 radicals and unimolecular decomposition at a ratio of 4:1 [10]. Both mechanisms show very good agreement with the measured values. In the UCL mechanism, a secondary path for benzene formation involving the formation of C_6H_7 from fulvene also contributes up to 10% in benzene destruction.

$C_4H_4 + C_2H_3 <=> C_6H_6$ (R39)
$C_6H_5 + H <=> C_6H_6$ (R40)
$C_6H_7 => C_6H_6 + H$ (R41)

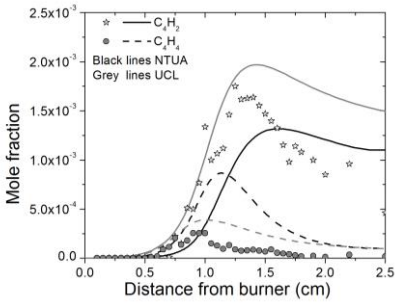

Figure 9 Comparison between experimental data (symbols), and computational results (lines) for C_4H_2 and C_4H_4 in Flame B.

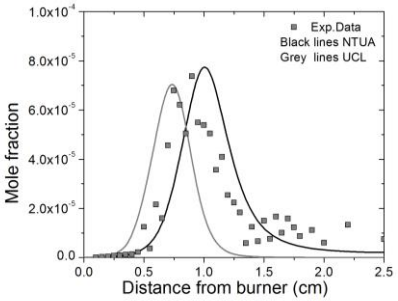

Figure 10 Comparison between experimental data (symbols), and computational results (lines) for C_4H_6 in Flame B.

Mechanisms performance against toluene data is shown in Fig. 12, where computations bracket the experiments. Toluene, is (exclusively in the NTUA mechanism, mainly in the UCL) formed through recombination reactions between phenyl and methyl radical and breaks directly to benzyl radical and a hydrogen atom.

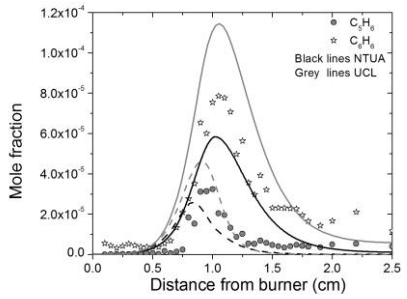

Figure 11 Comparison between experimental data (symbols), and computational results (lines) for C_5H_6 and C_6H_6 in Flame A.

The UCL mechanism adds a secondary C_7H_8 formation path, involving the reaction of hydroxyl with benzyl. Toluene is then destructed by hydrogen abstraction reactions forming again benzyl.

$C_7H_8 <=> C_6H_5+CH_3$ (R42)
$C_7H_8 <=> C_7H_7+H$ (R43)

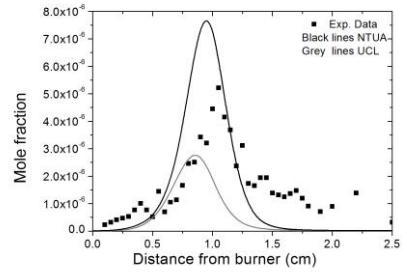

Figure 12 Comparison between experimental data (symbols), and computational results (lines) for C_7H_8 in Flame A.

Conclusions

The present work provides for the first time, a comprehensive investigation of the effect of the addition of oxygenated dopants to a rich ethylene flame. Combined novel experimental and numerical analyses was performed. Comparison between two detailed and well validated kinetic models for the combustion of small hydrocarbons was carried out. Results yielded good agreement for both mechanisms with some small discrepancies in peak levels and in reaction paths. It is concluded that Flames A and B maintain an oxygenated character throughout the flame domain, while at the same time the early shedding of CO_2 molecule in Flame C results in an apparent resemblance to an ethylene flame. Moreover, benzene levels in Flame C are found to be noticeably higher than in the other two flames. Additionally it has been found that the acetaldehyde levels in Flames A and B are significantly higher than in Flame C. This constitutes an interesting finding, considering the fact that despite the progress in engine aftertreatment, there is a lack in the respective technology for aldehydes. The study recognizes the need for measurements of global combustion characteristics such as ignition time delay and flame velocity for purposes of further understanding.

Acknowledgements

The NTUA authors and G. Skevis are grateful to the EU Marie Curie ITN for the financial support through the ECCO-MATE project (Grant No 607214). N. Leplat is grateful to the FRIA (Fonds pour la formation à la Recherche dans l'Industrie et dans l'Agriculture) for the financial support.

References

[1]. C.K. Law, AIAA J. 50 (2012) 19–36.
[2]. F. Battin-Leclerc, E. Blurock, R. Bounaceur, R. Fournet, P.A. Glaude, O. Herbinet, B. Sirjean, V. Warth, Chem. Soc. Rev. 40 (2011) 4762–4783.
[3]. S. M. Sarathy, P. Oßwald, N. Hansen, K. Kohse-Höinghaus, Prog. Energy Combust. Scie., 44 (2014), 40-102
[4]. E. Zervas, X. Montagne, J. Lahaye, Environ. Sci. Technol. 35 (2001) 2746–2751.
[5]. E. Zervas, X. Montagne, J. Lahaye, Tech. Chron. Sci. J. TCG 5 (1–2) (2004) 49–58.
[6]. M. Frenklach, Phys. Chem. Chem. Phys. 4 (2002) 2028–2037.
[7]. S.A. Yakimov, D.A. Knyaz'kov, T.A. Bol'shova, A.G. Shmakov, O.P. Korobeinichev, F. Qi, Combust Explo Shock+, 48 (2012) 609–619.
[8]. H. Xu, C. Yao, G. Xu, Z. Wang, H. Jin, Combust. Flame 160 (2013) 1333–1344
[9]. G. Vourliotakis, G. Skevis, M.A. Founti, Proc. Combust. Inst. 35 (2015), 437-445
[10]. G. Vourliotakis, G. Skevis, M.A. Founti, Energy Fuels 25 (2011) 1950–1963
[11]. N. Leplat, J. Vandooren, Combust. Flame 159 (2012) 493–499
[12]. N. Leplat, A. Seydi, J. Vandooren, Combust. Sci. Technol. 180 (2008) 519–532
[13]. N. Leplat, J. Vandooren Combust. Sci. Technol. 182 (2010) 436–448
[14]. N. Leplat, P. Dagaut, C. Togbé, J. Vandooren, Combust Flame, 158 (2011) 705–725
[15]. V. Detilleux, J. Vandooren, Combust. Explos. Shock Waves 45 (2009) 392-403.
[16]. V. Detilleux, J. Vandooren, Proc. Combust. Inst. 33 (2011) 217-224.
[17]. R.J. Kee, F.M. Rupley, J.A. Miller PREMIX: One-Dimensional Premixed Laminar Flame Code, CHEMKIN-II Version 2.5b, Sandia Laboratories, Livermore, CA, USA (1992)
[18]. V. Dias, J. Vandooren Combust Flame 158 (2011) 848–859
[19]. A. Bhargava, P.R. Westmorland Combust Flame 115 (1998) 456–467
[20]. R.P. Lindstedt, G. Skevis, Proc. Combust. Inst. 28 (2000) 1801–1807
[21]. C. Xu, A.A. Konnov, Energy 43 (2012) 19-29
[22]. A. Matsugi, A. Miyoshi, Int J Chem Kin, 46 (2014) 260-274.
[23]. W.K. Metcalfe, S.M. Burke, S.S. Ahmed, H.J. Curran, Int. J. Chem. Kinet. 45 (2013) 638–675.
[24]. H.R. Zhang, E.G. Eddings, A.F. Sarofim, C.K. Westbrook, Proc. Combust. Inst. 32 (2009) 377-385.